Article

Fe-Zeolite Catalysts Synthesized via Hydrothermal Method for Selective Catalatalytic Reduction of NOx with Ammonia

Chen Chen *

Posted Date: 5 January 2026

doi: 10.20944/preprints202601.0204.v1

Keywords: Fe-ZSM-5; selective catalytic reduction (SCR); hydrothermal synthesis; temperature-programmed desorption (TPD) doi:10.20944/preprints202601.0204.v1

Article

Fe-Zeolite Catalysts Synthesized via Hydrothermal Method for Selective Catalatalytic Reduction of NOx with Ammonia

Chen Chen

Jiangsu Aviation Technical College, Zhenjiang, Jiangsu 212134, China; 334124688@qq.com

Abstract

A series of Fe-ZSM-5 catalysts with varying Fe loadings were synthesized via a hydrothermal method. Their catalytic performance was evaluated for the selective catalytic reduction (SCR) of NOx with ammonia. The catalyst with a Fe:Al molar ratio of 1:1 demonstrated the highest NOx conversion (99.9%) and exhibited a broader operating temperature window (240–390 °C) compared to catalysts with other Fe/Al ratios. Characterization by X-ray diffraction (XRD),scanning electron microscopy(SEM), and X-ray photoelectron spectroscopy(XPS) confirmed that the incorporation of iron ions preserved the high crystallinity and MFI structure of the ZSM-5 zeolite. NH_3-temperature-programmed desorption (NH_3-TPD) profiles revealed the presence of two distinct acid sites at approximately 250 °C and 400 °C.

Keywords: Fe-ZSM-5; selective catalytic reduction (SCR); hydrothermal synthesis; temperature-programmed desorption (TPD)

1. Introduction

Iron-containing ZSM-5 zeolites (Fe-ZSM-5) have garnered significant attention as catalysts for the selective catalytic reduction (SCR) of NO_x (including NO and NO_2) with ammonia or hydrocarbons, as well as for N_2O decomposition/reduction [1–4]. These catalysts exhibit high resistance to SO_2 and H_2O poisoning under SCR conditions [1,5–8]. Furthermore, Fe-ZSM-5 catalysts typically operate within a broad temperature window, selectively produce N_2 and H_2O without significant N_2O byproduct formation, and show low activity for the undesirable oxidation of SO_2 to SO_3 [9].

Conventional preparation methods for Fe-ZSM-5 include ion exchange and wet impregnation [10–13]. However, these methods often suffer from poor reproducibility and can lead to the formation of large iron oxide particles upon calcination. Chemical vapor deposition (CVD) using gaseous $FeCl_3$ has been shown to be an efficient and reproducible technique for achieving high dispersion of extra-framework iron at the exchange sites of the ZSM-5 lattice [12]. Crucially, the active species in these catalysts are typically formed only after high-temperature treatment of the as-synthesized materials [11,15]. Alternatively, hydrothermal synthesis offers a direct route for incorporating iron into the zeolite framework. For instance, the group of J.B. Taboada [15] demonstrated the synthesis of ZSM-5 zeolites enriched with the ^{57}Fe isotope, where iron was present as well-distributed Fe^{3+} ions within the framework.

Despite extensive research, the nature of the active sites in Fe-ZSM-5 catalysts remains a topic of debate. Conventionally prepared Fe-ZSM-5 catalysts often require operating temperatures above 400 °C to achieve high activity, with maximum NO_x conversions typically around 90%. However, the influence of iron content introduced via direct hydrothermal synthesis on SCR activity has been less explored. This work aims to systematically investigate the effect of the Fe/Si ratio in catalysts synthesized in-situ by hydrothermal method. The primary objective is to modulate the acidity of the

Fe-ZSM-5 catalysts to enhance their low-temperature SCR activity, lower the operating temperature, and widen the effective temperature window.

2. Experimental

2.1. Catalyst Preparation

A series of Fe-ZSM-5 catalysts were produced hydrothermally. Zeolites were synthesized using solution of $NaAlO_2$, TEOS, Fe $(NO_3)_3 \cdot 9H_2O$ and NaOH. Tetrapropyl ammonium bromide was used as template and mobilizing agent. The starting mixtures were formed using the following procedures:

n Na_2O: nSiO_2: n ($NaAlO_2$+Fe $(NO_3)_3$): n TPABr: nH_2O=12: 70: 1: 45: 7000.

$NaAlO_2$ was first dissolved in water to get solution A, into which NaOH solution was added. TEOS, TPABr and Fe $(NO_3)_3 \cdot 9H_2O$ were added to deionized water, and solution were added to above solution slowly while stirring.

The reagent mixture was prepared by intensive stirring of the initial reagents for 5 h. And then the resulting solution aged 12 h.

Crystallization was carried out at a constant temperature of 170°C in a steel rotational autoclave for a period of 24 h. After that, the solid phase was filtered from the mother solution, washed several times with distilled water until it had a pH of 7. It was dried at a temperature of 100°C and calcined at 550°C for a period of 6 h to remove template and other impurities. Using the procedure, different zeolites with Fe: Al=0:1, 1:2, 1:1, 3:1 and 1:0 for Si/ (Fe+Al) =35 were synthesized.

2.2. Catalyst Characterization and Activity Measurements

X-ray diffraction measurement was performed on a Bruker D8 Advance X-ray diffraction using Cu Kα radiation in the 2θ interval 5-50°.

The scanning electron microscope image was obtained on LEO-1530VP scanning electron microscope. SEM images were recorded on samples with deposited Au for improved conductivity.

The BET surface areas (S_{BET}) and pore volumes (V_{pore}) of the Fe-ZSM-5 catalyst were determined by surface area and pore porosimetry analyzer (V-Sorbet 2008S). The sample was in vacuum at 150°C prior for 8 hs to measurement. And then the sample was measured by using N_2 adsorption at -196°C.

X-ray photoelectron spectroscopy analysis was performed in ESCA PHI 5000C System. Al/Mg radiation (14.0kV, 250W) was used to excite photoelectrons.

Temperature-programmed desorption (NH_3-TPD and NO-TPD) measurements were performed using a Chembet PULSAR TPR/TPD fully automated dynamic chemisorption analyzer manufactured by Quantachrome Instruments (USA). The NH_3-TPD (NO-TPD) experiment was performed by the following procedure: 150 mg of calcined sample was loaded into a quartz tube reactor, pre-treated by heating in a flowing stream of argon, heated from room temperature to 60°C at 10°C$\cdot$min^{-1} and stayed at 60°C for 1 h. This was done to remove water and desorb unwanted impurities. After that, the argon flow was switched to a flow of NH_3/N_2 1.94 vol. % or (NO/N_2 1.00vol. %) for about 1 h until the signal was steady. The catalyst was saturated with NH_3 (NO). Prior to NH_3 (NO) desorption measurement, the sample was swept by a flow of dry argon (70mL$\cdot$min^{-1}) for 1 h to remove physically adsorbed NH_3 (NO). Desorption was carried out at a heating rate of 15°C$\cdot$min^{-1} from 60°C to 700°C in a He flow (70mL $\cdot$min^{-1}).

The SCR activity measurement was carried out in a fixed-bed. A sample of 1g Fe-ZSM-5 catalyst (crushed to powder and sieved to 20-40 mesh) was loaded in a fixed-bed. The reaction temperature was controlled by programmable temperature controller. The total flow rate was 100mL$\cdot$min^{-1} (ambient conditions), and the gas hourly space velocity (GHSV) was 6000mL$^{3}\cdot$g$_{cat}^{-1}\cdot$h^{-1}. The typical reactant gas composition was as follows: the balanced gas N_2, 450ppm NO, 450ppm NO_2, 1000ppm NH_3 and 6% O_2. The concentration of NO and NO_2 was continually monitored by the coal gas analyzer (Germany ECOM-JZKN). The NO and NO_2 conversion was obtained from the difference in the NOx concentrations before and after the SCR reaction,the formula of the NOx conversion is:

$$\eta=(NO_{X,in}-NO_{X,out})/NO_{X,in}\times100\%$$

doi:10.20944/preprints202601.0204.v1

SO_2 and H_2O resistance experiment was conducted in the same fixed-bed. A reaction mixture containing 450ppm NO, 450ppm NO_2, 1000ppm NH_3 , 600ppm SO_2 (5%H_2O) and 6%O_2 balanced with N_2 at a flow rate 100mL·min^{-1} (ambient conditions) was used.

3. Results and Discussion

Previously based on the conclusions of in situ FTIR studies, Long and Yang [16] has came up with the reaction mechanism of NOx SCR with ammonia over Fe-ZSM-5 catalysts shown in Figure 1. The SCR reaction needs two kinds of sites: the Brönsted acid sites for ammonia adsorption and the metal ion sites (i.e., Fe^{3+} ions) for NO oxidation to NO_2, a possible reaction mechanism is proposed for NO reduction involving NO_2 and $NO_2(NH_4^+)_2$ as intermediates. According to this mechanism, first and rate determining step for the SCR reaction is the oxidation of NO to NO_2 on Fe^{3+} sites by O_2, while gaseous NH_3 molecules are adsorbed quickly onto the Brönsted sites to form NH_4^+ ions. Subsequently, each NO_2 molecule reacts with two adjacent NH_4^+ ions to form the active complex, $NO_2(NH_4^+)_2$. The small pore size in ZSM-5 facilitates the formation of this complex, which produce N_2 and H_2O.

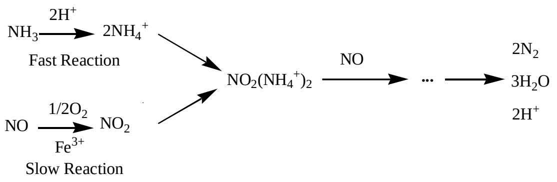

Figure 1. Reaction scheme of SCR of NO with ammonia on Fe-ZSM-5.

3.1. X-Ray Diffraction and Specific Surface Area

XRD patterns of different iron content ZSM-5 catalysts are very similar (Figure 2). These patterns were obtained after the zeolite catalyst synthesis and subsequent combustion of organic template. The same peaks appeared at 7.8°, 8.8°, 23.1°, 26.6° and 29.2°. All the Fe-ZSM-5 exhibited the typical lines of MFI framework, showed that all have a ZSM-5 structure with a high degree of crystallinity after Fe loading. All samples do not show any evidence of extra framework crystalline compounds or long-range amorphization of the zeolite catalyst.

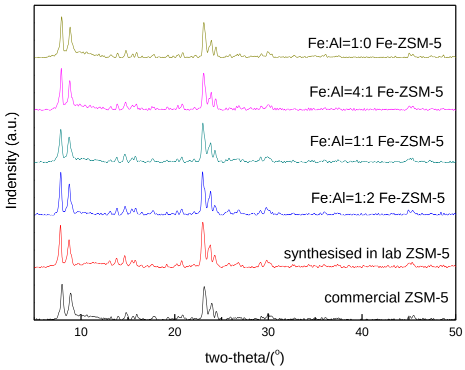

Figure 2. X-ray diffractograms recorded at room temperature and ambient atmosphere of different iron content ZSM-5.

We also observed that for samples with varying iron content, the diffractograms exhibit Bragg peaks around 7.8° and 8.8° 2θ (see inset in Figure 3), when the Fe: Al=1:0 ZSM-5 catalyst comparing with the Fe: Al=0:1 ZSM-5 catalyst, respectively indicates expansion of the matrix and suggests that iron was incorporated into the framework. We analyze that the radius of Fe^{3+} (0.067nm) is bigger than Al^{3+} (0.057nm), leading cell parameter a_0 to become larger. These slight differences in the XRD pattern are attributed to ZSM-5 crystals with varying amounts of iron, which causes the unit cells to vary in size (the length of Fe-O bond (1.86±0.1Å)) [16] is larger than that of Al-O bond (1.73 Å) and Si-O bond (1.63 Å) [17] and thus might induce small shifts of the Bragg peaks.

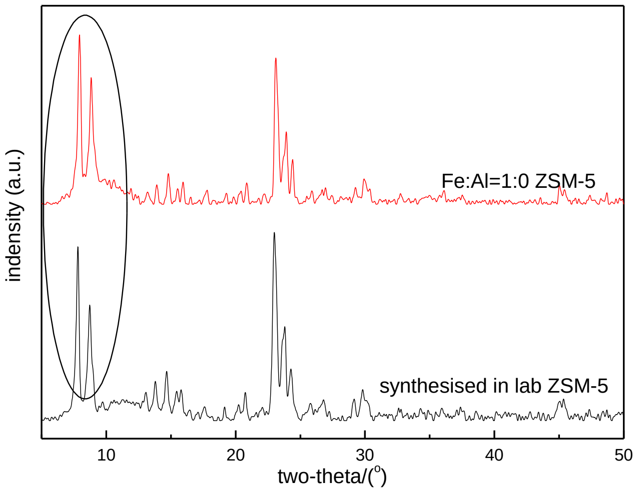

Figure 3. X-ray diffractograms recorded at room temperature and ambient atmosphere of Fe: Al=1:0 and Fe: Al=0:1 ZSM-5.

From the results of Fe: Al=1:1 Fe-ZSM-5 catalyst specific surface area test, we conclude that the BET specific surface area is 338m²·g⁻¹, Langmuir specific surface area is 446.04930 m²·g⁻¹. The diameter of pore is 0.58nm, which is typical for microporous materials.

3.2. Scanning Electron Microscope and X-Ray Photoelectron Spectroscopy

In Figure 4, it is show that the zeolite catalyst has formed nanoparticles with an average size between 1 and 3 µm which are named nanocrystalline. Besides, the surface of nanoparticles is very smooth, and there are no Fe_2O_3 particles in the surface of the zeolite catalyst.

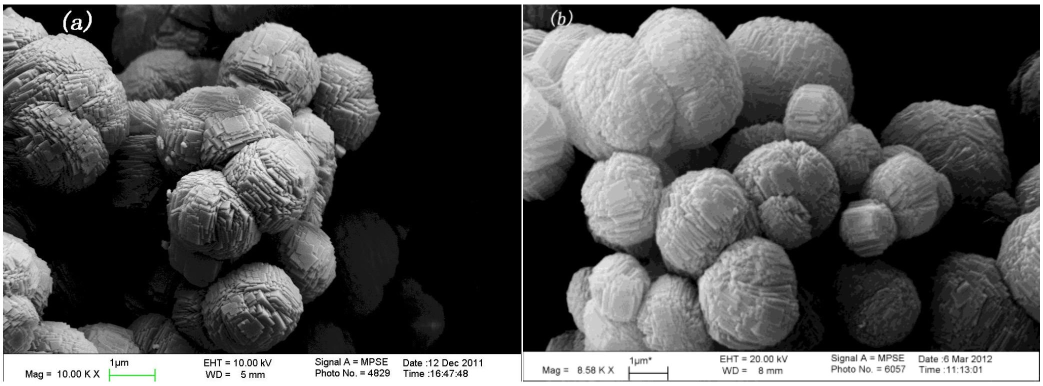

Figure 4. SEM images of samples. (a) Fe: Al=1:0 Fe-ZSM-5 catalyst; (b) Fe: Al=1:1 Fe-ZSM-5 catalyst.

On the basis of XPS spectra (Figure 5) measured on Fe-ZSM-5 (Fe: Al=1:1, prepared by hydrothermal method), it is found that the binding energies of $Fe2p_{3/2}$ photoelectron are between 711.6eV and 712.4eV. The value are higher than those for bulk α-Fe_2O_3 (710.5 [18], 711.2 eV [19]) and Fe_3O_4 (710.5 [20], 711.2 eV [18]). This may indicate a strong interaction between iron and zeolite, and in fact, the binding energies of 711.6 and 712.1-711.4 eV are reported for iron incorporated in Fe-ZSM-5 [20] and Fe_2O_3-SiO_2 [21].

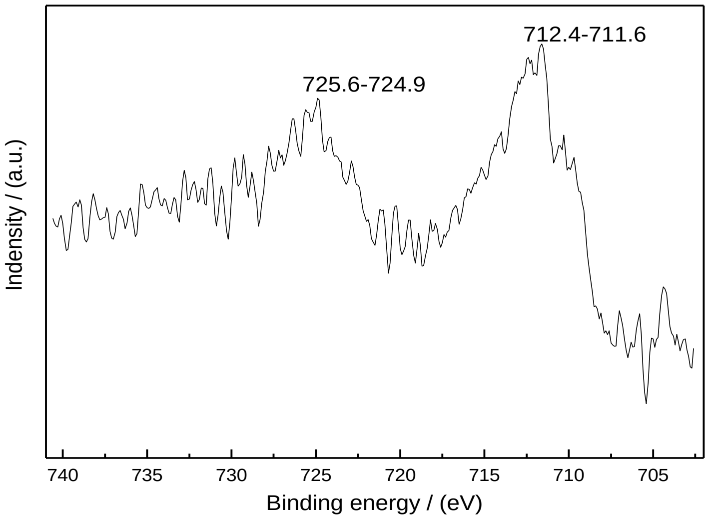

Figure 5. XPS spectra of Fe2p over Fe: Al=1:1 Fe-ZSM-5catalyst.

In Figure 6 (1) and (2), they show Si2p and O1s spectra obtained over Fe: Al=0:1 and 1:1 Fe-ZSM-5. The main peaks of Si2p and O1s over Fe: Al=1:1 Fe-ZSM-5 are both slightly smaller than that for Fe: Al=0:1 Fe-ZSM-5. It may indicate that Fe was incorporated into the framework and formed Fe-O-Si. The electronegativity of Fe is smaller than Al, so that the main peak shifts to low binding energy. These findings are supported by the X-ray powder diffraction and scanning electron microscope.

Iron in the framework sites is essentially in tetrahedral oxygen coordination. On the other hand, iron in the extra framework sites is probably present as iron oxide clusters, which are likely to occupy the octahedral sites such as those observed in the bulk phases of α-FeOOH (goethite) and α-Fe_2O_3 (hematite). Moreover, the XPS of the catalysts, exhibited no other little peaks expect Fe^{3+} ions in Figure 5. This indicates that all iron must be in the framework position since the Fe^{3+} ions in the framework are hard to reduce, in agreement with previous studies [15].

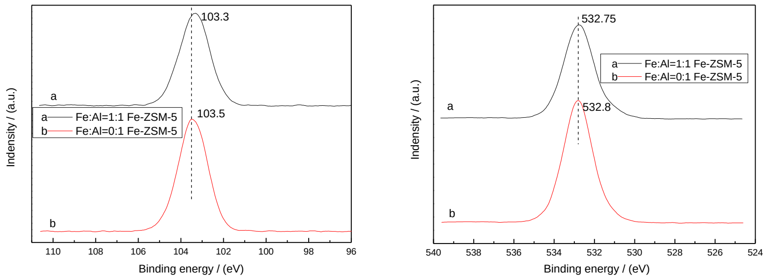

(**a**) (**b**)

Figure 6. XPS spectra of (a) Al 2p obtained over Fe-ZSM-5 (b) Si 2p obtained over Fe-ZSM-5 catalysts.

3.3. Temperature Programmed Desorption of Ammonia (NH_3-TPD)

Acidity and pore structure of ZSM-5 catalysts are main factors affecting the catalytic properties. It is concluded that the introduction of iron will not damage the skeleton structure of molecular sieve from the previous results of XRD characterization, and the pore structure of the zeolite catalyst does not change. In order to investigate the introduction of iron effect on the zeolite catalyst acidity, the NH_3-TPD measurements were performed for catalysts of different iron content.

According to the results of ammonia-TPD (Figure 7), introduction of iron leads to the decrease of the total amount of desorbed ammonia in all cases. For Fe-ZSM-5 catalysts, the intensity of the peak is lower than that of Fe: Al=0:1 Fe-ZSM-5, because the Brönsted acid protons were substituted by Fe^{3+}. At the same time, the total amount of acidity decreases slightly when the Fe/Al ratios increases. It indicates that Al adsorbed ammonia more easily than Fe, so Al adsorbed ammonia firstly and then Fe followed.

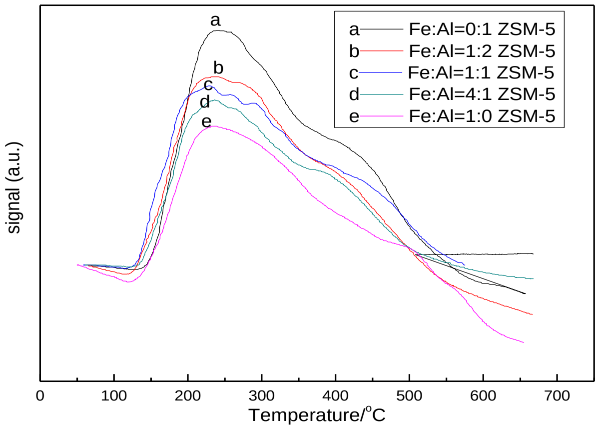

Figure 7. Temperature-programmed desorption of NH_3 over different iron content Fe-ZSM-5 catalysts.

The Figure 8 shows the comparison of Fe: Al=4:1 and Fe: Al=0:1 Fe-ZSM-5 catalyst, two different desorption peaks. The peak around 240℃ is due to desorption of weakly bound NH_3 followed by desorption around 400℃ due to strongly bound NH_3. The strongly bound NH_3 is arising from Fe-ZSM-5 unoccupied Brønsted hydroxyl groups and strong Lewis iron sites. The significant decrease in NH_3 desorption in the Fe: Al=4:1 Fe-ZSM-5 catalyst implies that Fe^{3+} is associated with ZSM-5 structure. It also shows that the center of the acidity sites shifts to the direction of low temperature when iron is introduced.

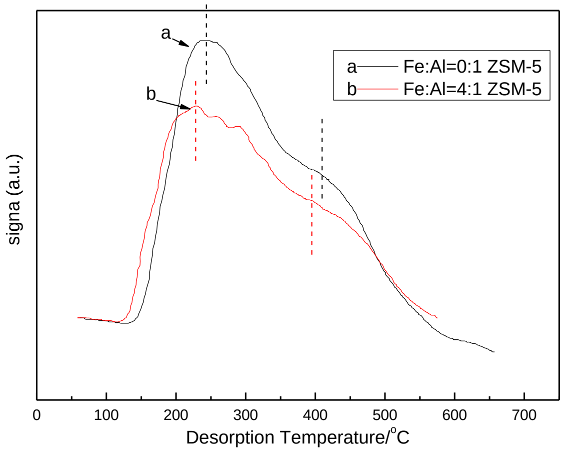

Figure 8. Temperature-programmed desorption of NH_3 over Fe: Al=0:1 and Fe: Al=4:1 ZSM-5 catalysts.

3.4. Temperature Programmed Desorption of Nitric Oxides (NO-TPD)

In Figure 9, the amount of NO adsorption of Fe: Al=1:1 zeolite catalyst is the largest among the different iron content zeolite catalysts. The result indicates that the Fe: Al=1:1 Fe-ZSM-5 catalyst adsorbed more NO than other different iron content between 250℃ and 350℃. As shown before, NH_3 is also adsorbed at 250℃, so the adsorbed NO could react with other molecules in the active acid sites.

For molecular sieve-type catalysts, it was reported that both NOx and NH_3 molecules could adsorb on the catalysts [22,23].

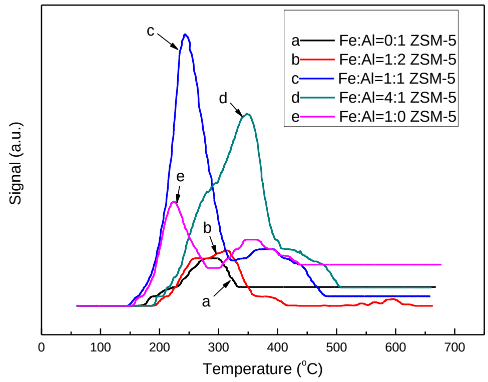

Figure 9. TPD spectra of NO desorption from different iron loaded ZSM-5 catalysts.

3.5. SCR Activity Testing

All catalysts used in this test were highly crystalline as determined by XRD and contained no trace impurities. BET showed that the Fe-ZSM-5 catalysts had microporous volumes consistent with the ZSM-5 structure. Iron was incorporated into the framework from the results of XPS, SEM and XRD. In some literature data, NO_2 may dissociate onto the red-ox sites. Meanwhile, monoxide would participate in the fast SCR path (for which a mixture of NO and NO_2 is required) [24]. The best DeNOx performances could be obtained always with NO_2/NOx ratios close to 0.5 [25].

Since the reaction temperature plays an important role in SCR of NOx, it is necessary to seek the optimum temperature window for the prepared Fe-ZSM-5 catalysts. The activity of the catalysts in the series is systematically investigated as shown in Figures 10–14.

The NOx conversion increases in all cases and passes through maxima as the temperature increased to 390°C. When the Fe: Al=1:1, the activity of the Fe-ZSM-5 catalyst is the most efficient catalyst. The NOx conversion between 240°C and 390°C is nearly 100%. Besides, the NOx window is shifted to the direction of lower temperature. The window of the Fe: Al=1:1 ZSM-5 catalyst is the widest (from 240°C to 390°C), and the conversion is almost 100%. The conversion of NO_2 is higher than that of NO over the Fe-ZSM5 catalysts, although a 1:1 mixture of NO and NO_2 was fed to the catalyst.

Moreover, we conducted a SO_2 and H_2O resistance experiment for the catalyst. This type of study is essential for initiating the practical use of the Fe-ZSM-5 catalysts for NOx removal with NH_3. Figure 15 shows the evolution of NO and NO_2 conversion over Fe: Al=1:1 Fe-ZSM-5 under different conditions with time on. Adding H_2O and SO_2 individually had almost no influence on NO and NO_2 conversion above 270°C to Fe: Al=1:1 Fe-ZSM-5. However, the conversion NOx decreased deeply, when H_2O and SO_2 were added at the same time. The above inhibitions could be reduced by increasing reaction temperature and were reversible.

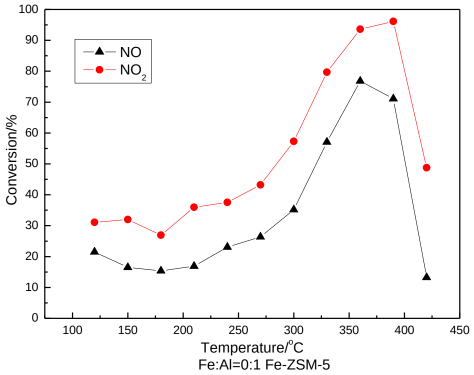

Figure 10. NO and NO2 reduction as a function of temperature over the Fe: Al=0:1 ZSM-5 catalyst.

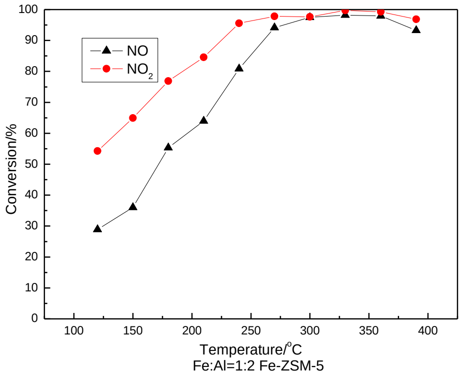

Figure 11. NO and NO2 reduction as a function of temperature over the Fe: Al=1:2 Fe-ZSM-5 catalyst.

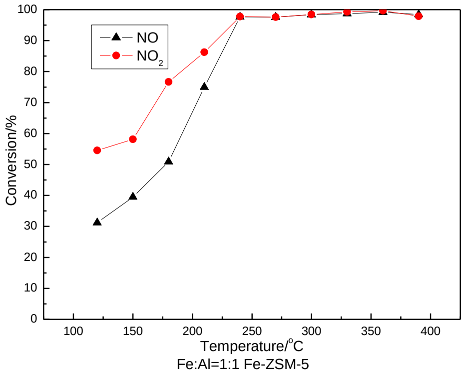

Figure 12. NO and NO2 reduction as a function of temperature over Fe: Al=1:1 Fe-ZSM-5 catalyst.

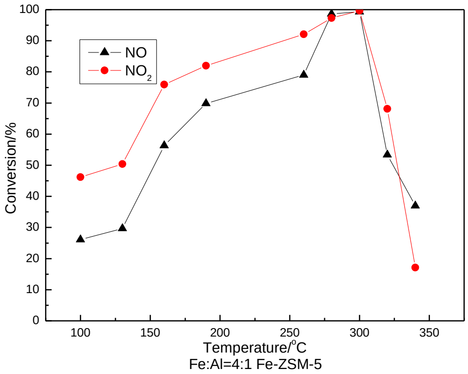

Figure 13. NO and NO2 reduction as a function of temperature over Fe: Al=4:1 Fe-ZSM-5 catalyst.

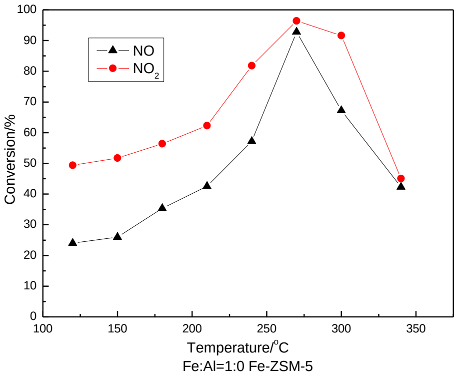

Figure 14. NO and NO_2 reduction as a function of temperature over Fe: Al=1:0 Fe-ZSM-5 catalyst.

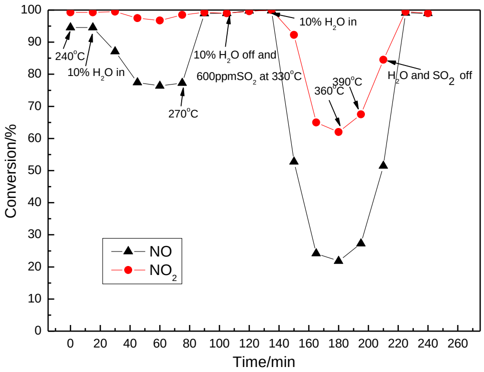

Figure 15. The evolution of NO and NO_2 conversion over the Fe: Al=1:1 Fe-ZSM-5 catalyst with time on.

4. Conclusions

A series of Fe-ZSM-5 catalysts with varying Fe/Al ratios were successfully synthesized via a one-pot hydrothermal method. Comprehensive characterization (XRD, XPS, SEM) confirmed the isomorphous substitution of Fe^{3+} ions into the zeolite framework, forming Fe–O–Si linkages. The catalyst with a Fe:Al molar ratio of 1:1demonstrated the highest catalytic activity, achieving nearly 100% NO_x conversion within a wide temperature window of 240–390 °C.NH_3-TPD studies revealed that iron incorporation modifies the acidity, reducing the overall acid amount and strength. NO-TPD results correlated with catalytic performance, showing the highest NO adsorption capacity for the Fe:Al=1:1 catalyst. The catalyst also showed good resistance to individual poisoning by H_2O or SO_2, though synergistic inhibition was observed when both were present. This work highlights the effectiveness of hydrothermal synthesis in creating highly active and durable Fe-ZSM-5 catalysts for low-temperature NH_3-SCR of NO_x.

Funding: Fund Project: “Research on the Construction of Aviation Emergency Rescue System from the Perspective of Low-altitude Economy” (2025SJYB1676), a 2025 Philosophy and Social Sciences Research Project of Universities in Jiangsu Province.

References

1. Shi X,Wang Y,Shan Y,et al.Investigation of the common intermediates over Fe-ZSM-5 in NH3-SCR reaction at low temperature by in situ DRIFTS[J].Journal of Environmental Sciences,2020,94(08):32-39.
2. Sun K Q, Xia H A, Hensen E, Santen R van, Li C. Chemistry of N_2O decomposition on active sites with different nature: Effect of high-temperature treatment of Fe/ZSM-5 [J]. Journal of Catalysis, 2006, 238: 186～195.
3. Pérez-Ramírez J. Active iron sites associated with the reaction mechanism of N_2O conversions over steam-actived FeMFI zeolites [J]. Journal of Catalysis, 2004, 227: 512～522.
4. Schwidder M, KumarM S, Klementiev K, et al. Selective reduction of NO with Fe-ZSM-5 catalysts of low Fe content I. Relations between active site structure and catalytic performance [J]. Journal of Catalysis, 2005, 231: 314～330.
5. Qi G, Yang R T. Ultra-active Fe/ZSM-5 catalyst for selective catalytic reduction of nitric oxide with ammonia [J]. Applied Catalysis. B Environmental, 2005 60: 13～22.
6. ZHANG Yu-bo,WANG Pan,YU Dan, et al.Evolution mechanism of active sites for NH_3-selective catalytic reduction of NO_x over Ce/Cu-doped Fe-ZSM-5 catalysts[J]. Journal of Central South University,2022,29(7): 2239-2252.
7. Long R Q, Yang R T. Selective catalytic oxidation (SCO) of ammonia to nitrogen over Fe-exchanged zeolites [J]. Journal of Catalysis, 2001, 201: 145～152.
8. Krishna K, Seijer G B F, Bleek C M van den, et al. Selective catalytic reduction of NO with NH_3 over Fe-ZSM-5 catalysts prepared by sublimation of $FeCl_3$ at different temperatures [J]. Catalysis Letter, 2003, 86: 121～132.
9. Long R Q, Yang R T. Temperature-programmed desorption/surface reaction (TPD/TPSR) study of Fe-exchanged ZSM-5 for selective catalytic reduction of nitric oxide by ammonia [J]. Journal of catalysis, 1999, 198: 20～28.
10. Li Z, Shen L, Huang W, et al. Kinetics of selective catalytic reduction of NO by NH_3 on Fe-Mo/ZSM-5 catalyst [J]. Journal of Environmental Science, 2007, 19: 1516～1519.
11. Zhou H,Liu J,Zhang Y, et al.Hydrothermal aging alleviates hydrocarbon poisoning effects on high-silica Cu-SSZ-16catalysts for NH3-SCR[J].Journal of Environmental Sciences,2025,158(12):13-23.
12. Delahay G, Valade D, Guzmán-Vargas A, et al. Selective catalytic reduction of nitric oxide with ammonia on Fe-ZSM-5 catalysts prepared by different methods [J].Applied Catalysis B: Environmental, 2005, 55: 149～155.
13. Kustov A L, Hansen T W, Kustova M, et al. Selective catalytic reduction of NO by ammonia using mesoporous Fe-containing HZSM-5 and HZSM-12 zeolite catalysts: an option for automotive applications [J]. Applied Catalysis B: Environmental, 2007, 76: 311～319.
14. Wang X,Chi R,Gu L,et al.Effect of water vapor on low temperature SCR performances over Cu and Mn-based catalysts:A comparison study[J].Journal of Rare Earths,2025,43(08):1661-1667.
15. Taboada J B, Oveweg A R, Crajé M W J, et al. Systematic variation of ^{57}Fe and Al content in isomorphously substituted and characterization [J]. Microporous and Mesoporous Materials, 2004, 75: 237～246.
16. Long R Q, Yang R T. Reaction mechanism of selective catalytic reduction of NO with NH_3 over Fe-ZSM-5 catalyst [J]. Journal of Catalysis,2002, 207: 224～231.

17. Berlier G, Spoto G, Bordiga S,et al. Evolution of extraframework iron species in Fe silicalite 1. Effect of Fe content, activation temperature, and interaction with redox agents [J].Journal of Catalysis, 2002, 208: 64～82.
18. Li H,Ren W,Xue H,et al.Significantly enhanced low-temperature activity and SO2/H2O tolerance of Mn-Ce-Ox/TiO2 catalysts prepared by a facile citric acid assisted impregnation method[J].Journal of Rare Earths,2025,43(06):1195-1204.
19. Brundle C R, Chuang T J, Wandelt K. Core and valence level photoemission studies of iron-oxide surfaces and oxidation of iron [J]. Surface Science, 1997, 68: 459～468.
20. Udovic T J, Dumesic J A. Preparation and characterization of magnetite surfaces on metallic iron substrates [J]. Journal of Catalysis, 1984, 89: 303～313.
21. Fabrizioli P, Bürgi T, Burgener M, et al. Synthesis, structural and chemical properties of iron oxide-silica aerogels [J] Journal of Materials Chemistry, 2002, 12: 619～630.
22. Chen H Y, Sachtler W M H. Activity and durability of Fe/ZSM-5 catalysts for lean burn NOx reduction in the presence of water vapor [J].Catalysis Today, 1998, 42: 73～83.
23. Long R Q, Yang R T. Characterization of Fe-ZSM-5 catalyst for selective catalytic reduction of nitric oxide by ammonia [J]. Journal of Catalysis, 2000, 194: 80～90.
24. Malpartida I, Marie O, Bazin P, et al. The NO/NOx ratio effect on the NH_3-SCR efficiency of a commercial automotive Fe-zeolite catalyst studied by operando IR-MS [J]. Applied Catalysis B: Environmental, 2012, 113-114: 52～60.
25. Colombo M, Nova I, Tronconi E. A comparative study of the NH_3-SCR reaction over a Cu-zeolite and a Fe-zeolite catalyst [J]. Catalysis Today, 2010, 151: 223～230.